arXiv:1406.1681v1 [physics.ao-ph] 6 Jun 2014

Deep-water gravity waves: nonlinear theory of wave groups

I. M. Mindlin
Department of Applied Mathematics, State Technical University,
Minina St., 24, Nizhny Novgorod 603155, Russia
E-mail address: ilia.mindlin@gmail.com

Nonlinear initial-boundary value problem on deep-water gravity waves of finite amplitude is solved approximately (up to small terms of higher order) assuming that the waves are generated by an initial disturbance to the water and the horizontal dimensions of the initially disturbed body of the water are much larger than the magnitude of the free surface displacement.

A numerable set of specific free surface waves is obtained in closed form and it is shown that free surface waves produced by an arbitrary initial disturbance to the water is a combination (not superposition: the waves are nonlinear) of the specific waves.

A set of dispersive wave packets is found with one-to-one correspondence between the packets and positive integers, say, packet numbers, such that any initial free surface displacement gradually disintegrates into a number (limited or unlimited, depending on initial conditions) of the wave packets. The greater the packet number, the shorter the wavelength of the packet's carrier wave component, the slower the packet travels, the slower the packet disperses; evolution of any of the packets is not influenced by evolution of any other one.

It is found that in case of infinitesimal wave amplitude the present theory is in agreement with linear wave theory. On the other hand, the behaviour of wave packets of large numbers and asymptotic behaviour of solutions of Schrödinger equation for weakly nonlinear waves are found to be similar, except for dispersion The theory is tested against experiments performed in a water tank.

Keywords. Deep water surface waves, weakly nonlinear waves, wave packets.

1. Introduction

1.1. Overview of the suggested approach

We present a theory of nonlinear deep-water waves in a vertical plane which start to propagate away from an initially disturbed body of water. Then the water is acted on by no external force other than gravity. It is assumed that the free surface of the water is infinite in extent and the pressure along the surface is constant.

Classical equations of the problem includes (i) the Laplace's equation for the velocity potential, (ii) nonlinear kinematic condition which means that a liquid particle in the free surface can have no velocity relative to the surface in

the direction of the normal, (iii) nonlinear condition of the pressure continuity across the free surface, (iiii) conditions at infinity, (iiiii) initial conditions.

In the available literature nonlinear analysis of deep water waves is based on Schrödinger equation for weakly nonlinear waves.

Assuming that the frequency, amplitude, and wave number of a weakly nonlinear evolving wave train are slowly varying functions of time, the classical equations for free surface gravity waves were reduced to equations governing the evolution of the frequency, amplitude, and wave number. These equations in turn were reduced to nonlinear Schrödinger equation for complex-valued wave envelope [1, 2, 3, 4].

Asymptotic behaviour of solutions of the Schrödinger equation was revealed by Zakharov & Shabat [5]. Provided the initial free surface displacement (away from the equilibrium position of the surface) decays sufficiently rapidly with distance from the maximum of the displacement, it was found, in particular, that an initial wave packet of arbitrary envelope shape disintegrates with time into a number of final packets, each of specific envelope shape, and an oscillating 'tail'; the envelope of each final packet is a solution of the Schrödinger equation; the number of final wave packets depends on initial conditions for the equation; the envelope of a final packet travels at a constant velocity, keeps its shape, and retains its shape and velocity after interaction with other final packets (this is the reason to use the term 'envelope soliton'). That is, the solitons do not disperse.

Disintegration of a wave packet into final packets travelling at different velocities is also the dispersion. But the final packets don't disperse. Why? Supposedly due to a dynamic balance between nonlinear and dispersive effects.

In any case, existence of the envelope solitons for solutions of Schrödinger equation does not assure the balance of nonlinearity and dispersion for solutions of classical equations for deep-water gravity waves.

A quite different approach to the initial-boundary value problem on the waves is developed in the article, based on the author's previous works [6, 7] .

The principal features of the suggested approach are:

- It is assumed that horizontal dimensions of the initially disturbed body of water are much larger than the vertical displacement of the free surface in the wave originating area.
- A nonlinear transformation of the equations is performed. The transformation maps the trace of the free surface in a plane of flow onto a half of a circle. The mapping allows us to use a discrete (with respect to spacial argument) set of functions instead of integral Fourier transform involving continuum of harmonic waves.
- It is also assumed that initial conditions can be expanded in trigonometric series convergent on the segment of the circle.
- Solution of the transformed equations is sought in the form of series in powers of small parameter, the ratio of the two linear dimensions of initial disturbance.

- Adopting the initial conditions in the form of trigonometric series, we express the free surface evolution in the form of parametric equations, which allow waves to steepen until overturning occurs.

- The solution is obtained under boundary conditions at infinity which require the energy supplied to the water by a source of disturbances to be finite. By the conditions, the plane waves should be expressed in terms of functions vanishing at infinity along the free surface. A complete numerable set of such functions is constructed in the article.

Thus, in the suggested approach, different from replacing the original equations with the Schrödinger equation and seeking the 'envelope solution',

- no assumptions are made about wave numbers, frequency spectrum or any other solution features.The assumptions concern only initial conditions.

- relatively small terms are omitted in the solution, not in the equations, since small terms in the equations may essentially influence the long time evolution of the solutions.

- no a-priory assumption about time evolution of the solution is made.

- the energy of the solution is always finite. Consequently, periodic waves on the free surface infinite in extent (including sinusoidal and progressive Stokes waves) are 'prohibited' by these conditions.

. 1.2. Brief overview of the resulting solutions

Solutions presented in this article describe waves expressed in terms of nonlinear combinations of specific wave packets. The packets are subject to dispersion. A wave group on the free surface is a mixture of finite or infinite (it depends on initial conditions) set of the specific wave packets, evolution of each packet in the mixture is not influenced by evolution of the others.

Though any specific packet disperses, it tends to keep its shape within a finite time interval which depends on the packet carrier wave length. The greater the packet's number, the longer the time interval. So, on a finite time interval, behaviour of the specific packets of large numbers seems to be similar to that of the "envelope soliton" solutions of the Schrödinger equation [5].

Applicability of the Schrödinger equation to deep water waves is substantiated by some results of experiments performed in a water tank [8]. But theoretical results of the manuscript are supported by the same experiments in no less extent. Moreover, the theoretical results of the manuscript are in extremely good quantitative agreement with the experiments presented in [9].

As a limit case of the nonlinear theory, equations for infinitesimal deep water waves are obtained with boundary conditions on the evolving free surface, and the solution to the equations is found in the form of linear superposition of wave packets.. If the boundary conditions are shifted from the evolving free surface

to the equilibrium position of the surface, the equations reduce to equations of classical linear theory of infinitesimal waves.

1.3. Article outline

This work is organized and presented in eleven sections. Problem outline, basic equations in curvilinear coordinates and solution to the equations (up to small terms of higher order) are presented in sections 2 - 6. The results of the theory are discussed in sections 7, 8, 9 and 10. Properties of the specific wave packets are described and illustrated in sections 7 and 8. In section 9, a set of infinitesimal linear wave packets are obtained as a limit of the set of nonlinear packets. In connection with the limit, we would like to draw special attention to the assertions 2 and 3 formulated at the end of sections 9 and 10 respectively.

In the section 10, the theory is tested against experimental results presented in Yuen & Lake [8] and Feir [9]. The test show quantitative agreement between theoretical predictions and the experimental measurements of some parameters of wave packets.

The possibility to obtain the higher-order approximation to the full nonlinear problem is discussed in section 11.

2. Problem outline.

Referring to figure 1 and assuming that the motion is two-dimensional, in the (x, y)-plane, consider flow of an ideal heavy uniform liquid of density γ; the x-axis is oriented upward and the y-axis in horizontal direction. We think of the liquid as being contained between two vertical planes (parallel to the (x, y)-plane) at a distance apart.

Let the curve Γ (in figure 1) be the trace of the free surface S in the (x, y) plane, $x = f < 0$, $y = 0$ be the coordinates of the pole O_1 of the polar coordinate system in the (x, y) plane, θ be the polar angle measured from the positive x-axis in the counterclockwise direction, t be the time. The external pressure, P_*, on the free surface is constant. The liquid fills the space below the free surface. The equilibrium position of the free surface is in horizontal plane $x = 0$.

To satisfy the Laplace's equation, the velocity potential Φ is sought in the form of a doublet distribution over the free surface:

$$\Phi(P) = \frac{1}{2\pi} \int_\Gamma \nu(Q) \frac{\partial}{\partial n} \left(\ln \frac{1}{r} \right) dl$$

where Q and P are two points in the (x, y)-plane; Q is a point on the curve Γ, point P does not belong to the curve, $r = |PQ|$ is the distance between the points, $\nu(Q)$ is the density of the doublets distributed over the curve Γ, dl is the infinitesimal element of the curve (Fig. 1). Notation $\partial/\partial n$ is used for directional derivative at the point Q in the orthogonal direction to the curve Γ (unit vector of the direction points in the region above the free surface).

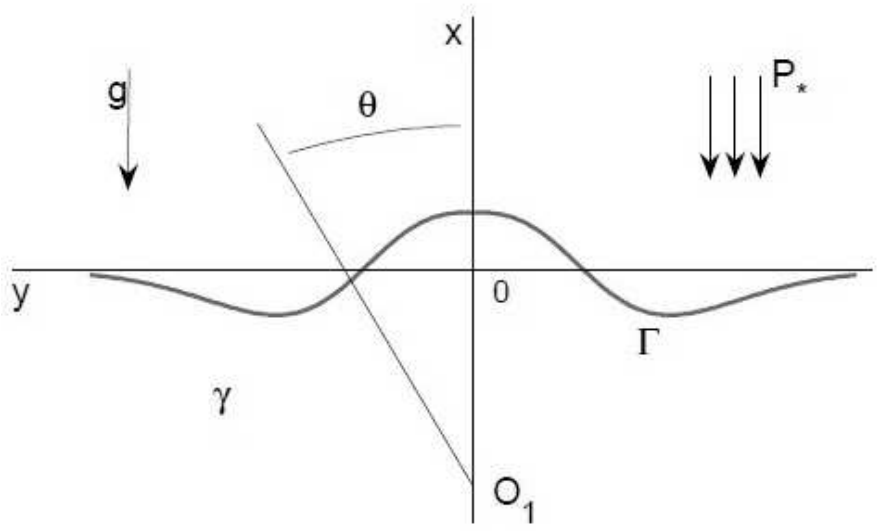

Figure 1: Coordinate systems and sketch of the free surface of a liquid.

Then the boudary-integral equation method is used: the classical differential equations accompanied by boundary conditions are reduced to a system of integrodifferential equations involving functions defined on the evolving free surface unknown in advance [10] .

3. Basic equations in curvilinear coordinates

Equations of the free surface are sought in the parametric form

$$x = W(\theta, t),\ y = (W - f)\ \tan\ \theta,\ -\pi/2 < \theta < \pi/2 \tag{3.1}$$

where $W(\theta, t)$ is an unknown function that must be found while solving the problem.

Formally, equations (3.1) for each specified function W describe a family of curves depending on f, t being considered as constant. The value of f determines the horizontal scale of the problem.

In the (x, y) plane, curvilinear coordinates (σ, θ) are defined by the relations

$$x = \sigma + W(\theta, t), \quad y = (\sigma + W - f)\ \tan\ \theta$$

so the equation of the free surface takes the form $\sigma = 0$ (the liquid occupies the half-space $\sigma < 0$).

All equations are rewritten in the curvilinear coordinates and the problem is formulated mathematically in terms of nonlinear integrodifferential equations in two unknown functions $W(\theta, t)$ and $\nu(\theta, t)$.

Note, that the change of variables is a nonlinear transformation of the equations written in Cartesian coordinates.

For any function $F(\sigma, \theta, t)$ the following notation is introduced for one-sided limit:

$$F_- = \lim_{\sigma \to -0} F(\sigma, \theta, t)$$

Velocity potential in curvilinear coordinates (σ, θ) is expressed as

$$\Phi(\sigma, \theta, t) = \frac{f}{|f|} \frac{1}{2\pi} \int\limits_{-\pi/2}^{\pi/2} \nu(\theta_1, t) A(\sigma, \sigma_1, \theta, \theta_1, t)\ \frac{d\theta_1}{R}\Big|_{\sigma_1 = 0} \tag{3.2}$$

$$A = (\sigma - \sigma_1 + W - W_1)(f - W_1) +$$

$$\frac{\sigma - f + W}{\sigma_1 - f + W_1}\ \frac{\partial W_1}{\partial \theta_1}\ (\tan\theta \cdot \cos^2\theta_1 - \sin\theta_1 \cdot \cos\theta_1)$$

$$R = (\sigma - \sigma_1 + W - W_1)^2 \cos^2\theta_1 +$$

$$[(\sigma - f + W)\tan\theta \cdot \cos\theta_1 - (\sigma_1 - f + W_1)\sin\theta_1]^2$$

$$W = W(\theta, t), \quad W_1 = W(\theta_1, t),$$

Equations (3.3) and (3.4) are nonlinear kinematic condition (ii) and nonlinear condition (iii) of the pressure continuity across the free surface $\sigma = 0$ respectively:

$$\frac{\partial W}{\partial t} = D_2 \frac{\partial \Phi}{\partial \sigma_-} - D_1 \frac{\partial \Phi}{\partial \theta_-} \tag{3.3}$$

$$\frac{\partial \Phi}{\partial t_-} - \frac{1}{2} D_2 \left(\frac{\partial \Phi}{\partial \sigma_-} \right)^2 + \frac{1}{2} \left(D \frac{\partial \Phi}{\partial \theta_-} \right)^2 + W(\theta, t) = 0 \tag{3.4}$$

$$D = \frac{\cos\theta}{W - f}, \quad D_1 = \left(\sin\theta + D \frac{\partial W}{\partial \theta} \right) D$$

$$D_2 = 1 + (D_1 + D \sin\theta) \frac{\partial W}{\partial \theta}$$

The conditions at infinity are taken in the form

$$|W(\theta, t)| < C(t) \cos^2\theta, \quad \lim_{\cos\theta \to 0} \frac{\partial W}{\partial \theta} = 0, \quad |\nu(\theta, t)| < C(t) \tag{3.5}$$

Although the liquid is infinite in extent, these conditions assure that the total energy supplied to the liquid by a source of disturbances is finite.

All equations are written in non-dimensional variables. Since the problem has no characteristic linear size, the dimensional unit of length, L_*, is a free parameter. But for applications in the section 10, the value of L_*, as well as the value of $|f|L_*$, will be obtained from instrumental data. The dimensional unit of time, T_*, is defined by the relation $T_*^2 g = L_*$, where g is the acceleration of free fall. The non-dimensional acceleration of free fall is equal to unity. All parameters, variables and equations are made non-dimensional by the quantities L_*, T_*, P_* and the density of water $\gamma_* = 1000$ kg/m^3.

4. Leading-order equations

Let c be the maximum of the free surface displacement in the wave origin, so $\varepsilon = c/f$ is the ratio of the maximum displacement to the characteristic horizontal dimension of the origin.

We seek expansions of the form

$$W(\theta, t) = c[W_0(\theta, t) + \varepsilon W_1(\theta, t) + ...], \quad \nu(\theta, t) = c \cdot [\nu_0(\theta, t) + \varepsilon \nu_1(\theta, t) + ...],$$

$$\Phi(\sigma, \theta, t) = c \cdot [\Phi_0(\sigma, \theta, t) + \varepsilon \Phi_1(\sigma, \theta, t) + ...]$$

By expanding all terms of the equations (3.2) - (3.4) in powers of ε and equating coefficients of like powers of ε we obtain the leading-order equations in unknown functions $W_0(\theta, t)$, $\nu_0(\theta, t)$, $\Phi_0(\sigma, \theta, t)$:

$$\frac{\partial \Phi_0}{\partial t_-} + W_0 = 0 \tag{4.1}$$

$$\frac{\partial W_0}{\partial t} = \frac{\partial \Phi_0}{\partial \sigma_-} + \frac{\sin\theta \cdot \cos\theta}{f} \frac{\partial \Phi_0}{\partial \theta_-} \tag{4.2}$$

$$\Phi_0(\sigma,\theta,t)=\frac{\sigma}{|\sigma|}H(\nu_0)$$

where the integral operator H is defined as follows

$$H(F(\theta))=|\alpha(1-\alpha)|\int\limits_{-\pi/2}^{\pi/2}\frac{F(\theta_1)\,d\theta_1}{a\cos^2\theta_1+b\sin^2\theta_1-c\sin(2\theta_1)}$$

$$\alpha=\frac{f}{f-\sigma},\quad a=(1-\alpha)^2+\tan^2\theta,\quad b=\alpha^2,\quad c=\alpha\ \tan\theta$$

Elemntary technique for analytic evaluation of integrals gives

$$2H(c_1\cos(2n\theta)+c_2\sin(2n\theta))=\mu_n(c_1\cos(2n\beta)+c_2\sin(2n\beta)) \tag{4.3}$$

$$\cos(2\beta)=\frac{2\alpha\cos^2\theta-1}{z},\quad \sin(2\beta)=\frac{\alpha\sin(2\theta)}{z}$$

$$\alpha=\frac{f}{f-\sigma},\quad z=\sqrt{1-4\alpha(1-\alpha)\cos^2\theta}$$

$$\mu_n=\frac{1}{z^n},\ \text{ if }\ \alpha(1-\alpha)<0$$

$$\mu_n=z^n,\ \text{ if }\ \alpha(1-\alpha)>0$$

With the use of (4.3), equations (4.1), (4.2) accompanied by boundary conditions (3.5) and initial conditions

$$W_0(\theta,0)=\cos^2\theta\sum_{n=1}^{+\infty}[a_n\cos(2n\theta)+b_n\sin(2n\theta)] \tag{4.4}$$

$$\nu_0(\theta,0)=\sum_{n=1}^{+\infty}[\rho_n\cos(2n\theta)+e_n\sin(2n\theta)]$$

can be solved exactly.

The constants a_n, b_n determine the initial displacement to the free surface, the constants ρ_n, e_n determine the initial velocity field.

The technique for handling the problem is described in [6]. The principal steps of the technique are shown in Appendix A.

5. Exact series solution to the leading-order equations

The exact solution of the problem (4.1), (4.2), (4.4), (3.5) was obtained in the form of functional double series [6]:

$$x=cW_0(\theta,t),\ y=(x-f)\tan\theta,\ \ -\pi/2<\theta<\pi/2 \tag{5.1}$$

$$W_0(\theta,t)=\sum_{n=1}^{+\infty}(-1)^{n-1}\frac{1}{2n}[a_nC_n(\tau,\theta)+b_nS_n(\tau,\theta)]+$$

$$\frac{1}{\sqrt{2|f|}}\sum_{n=1}^{+\infty}(-1)^n[\rho_nH_n(\tau,\theta)+e_nG_n(\tau,\theta)] \tag{5.2}$$

$$\frac{\partial\nu_0}{\partial t}=2W_0(\theta,t),\quad t=\tau\sqrt{2|f|}$$

where

$$C_n(\tau,\theta)=-2\cos^2\theta\cdot\sum_{k=1}^{+\infty}(-1)^k l_{kn}(\tau)\cos(2k\theta) \tag{5.3}$$

$$S_n(\tau,\theta)=-2\cos^2\theta\cdot\sum_{k=1}^{+\infty}(-1)^k l_{kn}(\tau)\sin(2k\theta) \tag{5.4}$$

$$H_n(\tau,\theta)=-2\cos^2\theta\cdot\sum_{k=1}^{+\infty}(-1)^k h_{kn}(\tau)\cos(2k\theta) \tag{5.5}$$

$$G_n(\tau,\theta)=-2\cos^2\theta\cdot\sum_{k=1}^{+\infty}(-1)^k h_{kn}(\tau)\sin(2k\theta) \tag{5.6}$$

$$l_{kn}(\tau)=2\int_0^{+\infty}x^3e^{-x^2}L_{k-1}^{(1)}(x^2)L_{n-1}^{(1)}(x^2)\cos(\tau x)\,dx \tag{5.7}$$

$$l_{kk}(0)=k,\quad l_{kn}(0)=0,\quad \text{for}\quad k\neq n$$

$$h_{kn}(\tau)=2\int_0^{+\infty}x^2e^{-x^2}L_{k-1}^{(1)}(x^2)L_{n-1}^{(1)}(x^2)\sin(\tau x)\,dx$$

The right hand side of (5.7) involves the Laguerre polynomials, $L_k^{(1)}(u)$, defined by the recursion relation [11]

$$L_0^{(1)}=1,\quad L_1^{(1)}(u)=2-u,\quad \text{for}\,k\geq 2$$

$$kL_k^{(1)}(u)=(2k-u)L_{k-1}^{(1)}(u)-kL_{k-2}^{(1)}(u) \tag{5.8}$$

Though the function $W_0(\theta,t)$ is a linear combination of solutions of linear equations (4.1), (4.2), the waves (5.1) are still nonlinear. In the wave theory, the principle of linear superposition states, in particular, that when two waves overlap, the actual displacement of any point of the free surface, at any time, is obtained by adding two displacements. The waves (5.1) does not obey the principle (the implicit form of the free surface is $x=cW_0(\text{arc tangent}(y/(x-f)),t)$).

6. Sum up of the series involved in the leading-order solution

Two theorems are formulated and proved in this section.

Theorem 1. In any rectangle $|\theta| \le \pi/2 - \delta$, $0 \le \tau \le T$, ($0 < \delta < \pi/2$, $T > 0$ may be assigned arbitrarily) series (5.3) through (5.6) converge uniformly with regard to θ and τ.

Theorem 2. On the interval $|\theta| < \pi/2$ the sums of the series are given by

$$C_n(\tau,\theta) = \int_0^{+\infty} x^3 e^{-x^2/2} L_{n-1}^{(1)}(x^2) \cos\phi \cos(\tau x)\, dx \tag{6.1}$$

$$S_n(\tau,\theta) = \int_0^{+\infty} x^3 e^{-x^2/2} L_{n-1}^{(1)}(x^2) \sin\phi \cos(\tau x)\, dx \tag{6.2}$$

$$H_n(\tau,\theta) = \int_0^{+\infty} x^2 e^{-x^2/2} L_{n-1}^{(1)}(x^2) \cos\phi \sin(\tau x)\, dx \tag{6.3}$$

$$G_n(\tau,\theta) = \int_0^{+\infty} x^2 e^{-x^2/2} L_{n-1}^{(1)}(x^2) \sin\phi \sin(\tau x)\, dx \tag{6.4}$$

where $\phi = 1/2\, x^2 \tan\theta$.

Proof of Theorem 1 essentially employs the asymptotic formula for Laguerre polynomials [11]

$$x^3 e^{-x^2} L_k^{(1)}(x^2) = \frac{1}{\sqrt{\pi}} k^{\frac{1}{4}} e^{-\frac{x^2}{2}} l_k \tag{6.5}$$

$$l_k = x^{\frac{3}{2}} \cos\left(2x\sqrt{k+1} - \frac{3}{4}\pi\right) + r_k$$

$$r_k = O\left(\frac{x^{\frac{1}{2}}}{\sqrt{k}}\right) + O\left(\frac{x^{\frac{9}{2}}}{\sqrt{k}}\right) + O\left(\frac{x^7}{k^{\frac{3}{4}}}\right) + h_k, \quad x \ge 0, \quad h_k = O\left(\frac{x^{\frac{3}{2}}}{k^{\frac{3}{4}}}\right)$$

where the notation $O(u)$ means 'of the order of u'.

The following Lemma is also used [5]:

Lemma. For $-\pi < \phi < \pi$ the following formula holds

$$s\sum_{k=1}^{+\infty} (-1)^k \frac{1}{k} L_{k-1}^{(1)}(s) e^{ik\phi} = 1 - \exp\left(\frac{1}{2}s\right) \cdot \exp\left(i\frac{1}{2}s\tan(\frac{1}{2}\phi)\right) \tag{6.6}$$

The series on the left side of (6.6) converges uniformly in any rectangle $|\phi| \le \pi - \delta$, $0 \le s \le s_0$ ($s_0 > 0$).

Proof of Theorem 1. When in the series (5.3) and (5.4) the products of trigonometric functions are decomposed into sums, the rearranged series take the form

$$\hat{C}_m(\tau,\theta) = -\frac{1}{2}\sum_{k=0}^{+\infty}(-1)^k \hat{l}_{km}(\tau)\cos(2k\theta) \tag{6.7}$$

$$\hat{S}_m(\tau,\theta) = -\frac{1}{2}\sum_{k=0}^{+\infty}(-1)^k \hat{l}_{km}(\tau)\sin(2k\theta) \tag{6.8}$$

$$\hat{l}_{km} = -l_{k+1,m} + 2l_{km} - l_{k-1,m}, \quad l_{-1,m} = l_{0,m} = 0$$

or, by (5.7) and (5.8),

$$\hat{l}_{0,m} = -l_{1,m}(\tau) = -2\int_0^{+\infty} x^3 B(x)\,dx$$

$$\text{for } k \geq 1 \;\; \hat{l}_{km}(\tau) = \frac{2}{k}\int_0^{+\infty} x^5 L_{k-1}^{(1)} B(x)\,dx \tag{6.9}$$

$$B(x) = \exp(-x^2) L_{m-1}^{(1)}(x^2)\cos(\tau x)$$

It follows from (5.7) and (6.5) that $l_{nm} = O(1/n^{1/4})$ for $0 \leq \tau \leq T$, where T and m are fixed.

The difference of the n-th partial sums of series (5.3) and (6.7) tends to zero as n tends to $+\infty$, since $l_{nm} \to 0$ as $n \to +\infty$. This means, that either both series converge to the same sum or both series diverge.

It follows from (6.5) and (6.9) that $\hat{l}_{nm} = O(1/n^{5/4})$. Now we conclude that series (6.7) converges absolutely and uniformly throughout the region $0 \leq \tau \leq T$, $|\theta| \leq \pi/2$ and series (6.5) converges uniformly in the same region.

The same result for series (5.4) - (5.6) can be proved in a similar manner. This completes the proof of Theorem 1.

Proof of Theorem 2. By the Lemma

$$x^2 \sum_{k=1}^{+\infty}(-1)^k \frac{1}{k} L_{k-1}^{(1)}(x^2)\cos(2k\theta) = 1 - \exp\left(\frac{1}{2}\,x^2\right)\cdot\cos\left(\frac{1}{2}\,x^2\cdot\tan\theta\right) \tag{6.10}$$

At any fixed value of θ, the series on the left side of (6.10) converges uniformly within any segment $0 \leq x \leq a$.

In the integral

$$\int_0^a x^3 e^{-x^2/2} L_{m-1}^{(1)}(x^2)\cos\left(\frac{1}{2}\,x^2\cdot\tan\theta\right)\cos(\tau x)\,dx$$

we replace the integrand with the series on the left side of (6.10) and perform the integration term by term. The integrals converge absolutely as $a \to +\infty$.

Letting a tend to $+\infty$, we obtain (6.7) and, consequently, (6.1).

Equalities (6.2) - (6.4) can be proved in the similar way.

In the proof of Theorm 1, it was found that the right-hand parts in (6.1) - (6.4) drop as $n^{-1/4}$. Series (5.2) converges absolutely, if values of a_n, b_n, ρ_n, and e_n drops, for example, as $1/n$.

Series (5.2) converges absolutely and uniformly with regard to θ and τ, if the initial free surface shape $W(\theta, 0)$ and initial doublet distribution $\nu(\theta, 0)$ are smooth functions and, consequently, can be expanded in a convergent Fourier series.

7. Specific wave packets

Theorem 3. The following expansions hold:

$$C_n(\tau,\theta) = \sum_{k=1}^{+\infty} 2^k\, k!\, b_{n,k}(\tau)(\cos\theta)^{k+1}\cos((k+1)\theta)$$

$$S_n(\tau,\theta) = \sum_{k=1}^{+\infty} 2^k\, k!\, b_{n,k}(\tau)(\cos\theta)^{k+1}\sin((k+1)\theta) \tag{7.1}$$

The coefficients $b_{n,k}(\tau)$ are defined by the following power series:

$$F_{n,1} \equiv x^2 L_{n-1}^{(1)}(x^2)\cos(\tau x) = \sum_{k=1}^{+\infty} b_{n,k}(\tau)(x^2)^k \tag{7.2}$$

In any rectangle $|\theta| \le \pi/2$, $0 \le \tau \le T$, ($T > 0$ may be assigned arbitrarily) series (7.1) converges uniformly with regard to θ and τ.

Similar expansions hold for $H_n(\tau, \theta)$ and $G_n(\tau, \theta)$.

Proof of Theorem 3. Write

$$C_m = \int_0^{+\infty} F_{m,1}\frac{\partial V_1}{\partial x}\,dx, \quad \frac{\partial V_1}{\partial x} = xe^{-x^2/2}\cos\phi$$

The function $F_{m,1}$ is defined by (7.2). In any rectangle $0 \le x \le a$, $0 \le \tau \le T$ series (7.2) converges uniformly with regard to x and τ.

Integration by parts gives

$$C_m = \cos\theta \cdot \int_0^{+\infty} F_{m,2}\frac{\partial V_2}{\partial x}\,dx$$

where

$$xF_{m,2} = \frac{\partial F_{m,1}}{\partial x}, \quad F_{m,2} = 2\sum_{k=1}^{+\infty} k b_{m,k}(\tau)(x^2)^{k-1}$$

$$\frac{\partial V_2}{\partial x} = xe^{-x^2/2}\left[\sin\theta\cos\phi + \cos\theta\sin\phi\right]$$

$$V_2 = -\cos\theta e^{-x^2/2}\left[\sin(2\theta)\cos\phi + \cos(2\theta)\sin\phi\right], \quad \phi = 1/2\, x^2\tan\theta$$

Performing the integration by parts again and again we come to the first equality (7.1). The second equality (7.1) can be proved in a similar manner.

It is not difficult to find that at any fixed value of m, coefficients $2^k k! b_{m,k}$ go to zero fast enough as $k \to +\infty$ to assure uniform convergence of series (7.1).

For $m = 1$ we have

$$F_{1,1} = x^2\cos(\tau x)$$

$$2^k k! b_{1,k} = (-1)^{k-1}\frac{2k}{(2k-3)!!}(\tau^2)^{k-1} \quad (k = 1,\, 2,\, \cdots)$$

$$(2k-1)!! = 1\cdot 3\cdot 5\cdot \ldots (2k-1), \quad (-1)!! = 0$$

If $m = 2$, then

$$F_{2,1} = x^2(2-x^2)\cos(\tau x)$$

$$2^k k! b_{2,k} = (-1)^{k-1}\frac{4k}{(2k-1)!!}(\tau^2)^{k-1} + (-1)^{k-1}\frac{4k(k-1)}{(2k-3)!!}(\tau^2)^{k-2}$$

Expression (7.1) shows that $W_0(\theta, t)$ satisfy boundary condition (3.5).

If in (7.1) coefficient $b_{m,1}$ does not equal zero, $W_0(\theta, t)$ drops as $1/y^2$ when y increases without bound. But the departure of the interface from its equilibrium position may drop faster: for any given natural number n and suitable initial conditions the departure drops as $1/y^{n+1}$ (and even faster). Indeed, there exist such value of λ_k that

$$u^n = \sum_{k=0}^{n} \lambda_k L_k^{(1)}(u)$$

so at initial conditions in (5.2) corresponding to λ_k we obtain $W_0(\tau, \theta) = I_{2n+1}$,

$$I_{2n+1}(\tau, \theta) = \int_0^{+\infty} x^{2n+1} e^{-x^2/2}\cos\phi\cos(\tau x)\, dx$$

In this case, expansion (7.2) should be replaced by

$$F(x) \equiv x^{2n}\cos(\tau x) = \sum_{k=n}^{+\infty} b_k(\tau)(x^2)^k$$

and, consequently,

$$I_{2n+1}(\tau, \theta) = \sum_{j=0}^{+\infty}(-1)^j\, 2^{n+j}\cdot(n+j)!\,\frac{\tau^{2j}}{(2j)!}(\cos\theta)^{n+1+j}\cos((n+1+j)\theta)$$

$$I_{2n+1}(0,\theta) = 2^n \cdot n!\,(\cos\theta)^{n+1}\cos((n+1)\theta)$$

The integral is normalized by $2^n \cdot n!$:

$$I_{2n+1}(\tau,\theta) = 2^n \cdot n!\,\hat{I}_{2n+1}(\tau,\theta), \quad \hat{I}_{2n+1}(0,0) = 1$$

$$\hat{I}_{2n+1}(0,\theta) = (\cos\theta)^{n+1}\cos((n+1)\theta)$$

Functions $C_m(\tau,\theta)$ are linear combinations of integrals $I_{2n+1}(\tau,\theta)$; for instance, $C_1(\tau,\theta) = I_3(\tau,\theta),\ C_2 = 2I_3 - I_5,\ 2C_3 = 2I_7 - 6I_5 + 6I_3$.

Similar results for $S_m(\tau,\theta)$, $H_m(\tau,\theta)$, and $G_m(\tau,\theta)$ can be obtained in the similar way.

We define spescific wave packets by equations

$$x = c_n I_{2n+1}, \quad y = (x-f)\tan\theta$$

$$I_{2n+1}(\tau,\theta) = \int_0^{+\infty} x^{2n+1} e^{-x^2/2}\cos(\frac{1}{2}x^2\tan\theta)\cos(\tau x)\,dx; \tag{7.3}$$

n is referred to as the packet number.

Equations of other three sets of wave packets will be obtained from (7.3) if the product of trigonometric functions in the integrand is replaced by one of the following expressions

$$\cos\phi\sin(\tau x)/x, \quad \sin\phi\cos(\tau x),$$

$$\sin\phi\sin(\tau x)/x, \quad \phi = \frac{1}{2}x^2\tan\theta$$

By equations (6.1), (6.2) and three Theorems, any wave group on the free surface is a mixture of finite or infinite (it depends on initial conditions) set of the specific wave packets of different numbers, and evolution of each packet in the mixture is not influenced by evolution of the others.

Zeros of the waves are defined by the equation $I_{2n+1}(\tau;\theta) = 0$ and (at fixed value of τ) are situated in the numbered rays $\theta = \theta_k(\tau)$ (k is the number of a zero). For brevity we will use the term 'zero $\theta(\tau)$' to denote a zero of a wave.

Zeros $\theta_k(\tau)$ of the wave packet (7.3) are independent of f and c_n.

Horizontal coordinate of the zero $\theta_k(\tau)$ is given by $y_k = -f\cdot\tan\theta_k(\tau)$. This leads to the following

Assertion 1: At any given value of τ

i) the vertical coordinates of the crests and the troughs (and, consequently, the waveheights) are independent of f;

ii) the ratio of the distances $y_{k+1}(\tau) - y_k(\tau)$ and $y_k(\tau) - y_{k-1}(\tau)$ between any successive zeros of the waves is independent of f.

In the course of time the number of zeros of the waves increases so the existence of the functions $\theta_k(\tau)$ on the whole semiaxis $\tau > 0$ is not assured.

Horizontal velocity of a zero of the wave is $dy_k/dt = u_k(\tau)\sqrt{0.5|f|}$, where $u_k(\tau) = d\tan\theta_k(\tau)/d\tau$.

The definition does not guarantee the existence of differentiable (and even continuous) functions $\tan\theta_k(\tau)$, but the average rate

$$u_k = [\tan\theta(\tau+\Delta\tau) - \tan\theta(\tau)]/\Delta\tau$$

exists, and this gives us a useful piece of information about the speed of waves as we will see in section 10.

Let L_* be the dimensional unit of length, then $T_* = \sqrt{L_*/g}$ is the dimensional unit of time.

At the instant t_* the dimensional coordinate of the zero $\theta = \theta(\tau)$ is

$$y_*(t_*) = |f|L_* \tan\theta(\tau), \quad t_* = \tau\sqrt{2|f|}\cdot T_*$$

and, consequently, the ratio

$$\lambda(\tau) = \frac{y_*(t_*)}{gt_*^2} = \frac{1}{2}\ \frac{\tan\theta(\tau)}{\tau^2} \tag{7.4}$$

depends on τ only.

Given a fixed value of τ, $\tan\theta(\tau)$ can be calculated from equations of a wave packet, and corresponding value of $\lambda(\tau)$ can be obtained from (7.4). Calculations show that $\tan\theta$ and λ are monotone functions of τ, so τ and $\tan\theta$ can be calculated for given value of λ.

At any particular moment of time, the system of waves contains only one wave of maximum height (WMH) on semiaxis $y > 0$ (the situation with two waves of equal maximum height can be ignored), so the zeros of WMH constitute a 'natural frame of reference' for other zeros.

The wave of maximum height is singled out by three zeros and consists of a crest and the trough following or preceding the crest. Let $\theta_r(\tau)$ and $\theta_f(\tau)$ denote two of the three zeros of the WMH which correspond to minimum and maximum of the three $|\tan\theta(\tau)|$ respectively. By the zero $\theta_f(\tau)$ we define the front of WMH at the instant τ, by $\theta_r(\tau)$ the rear of the wave is determined.

8. Evolution of specific wave packets

The figures 2 - 6 illustrate evolution of wave profiles specified by equations (at $f = -10$)

$$x = 0.4\,\hat{I}_{23}(\tau,\theta) + 0.075\,\hat{I}_5(\tau,\theta), \quad |y| = (x-f)|\tan\theta| \tag{8.1}$$

$$x = 0.4\,\hat{I}_{23}(\tau,\theta), \quad |y| = (x-f)|\tan\theta| \tag{8.2}$$

$$x = 0.075\,\hat{I}_5(\tau,\theta), \quad |y| = (x-f)|\tan\theta| \tag{8.3}$$

At each value of τ, the profiles are drawn in the same scale. For each of the profiles, initially,jpgjpg at $\tau = 0$, the crest of the wave of maximum height is situated on the ray $\theta = 0$, i.e., on the x-axis; the vertical coordinates of the crests are: $x = 0.4$ for (8.2), $x = 0.075$ for (8.3), and, consequently, $x = 0.475$ for (8.1).

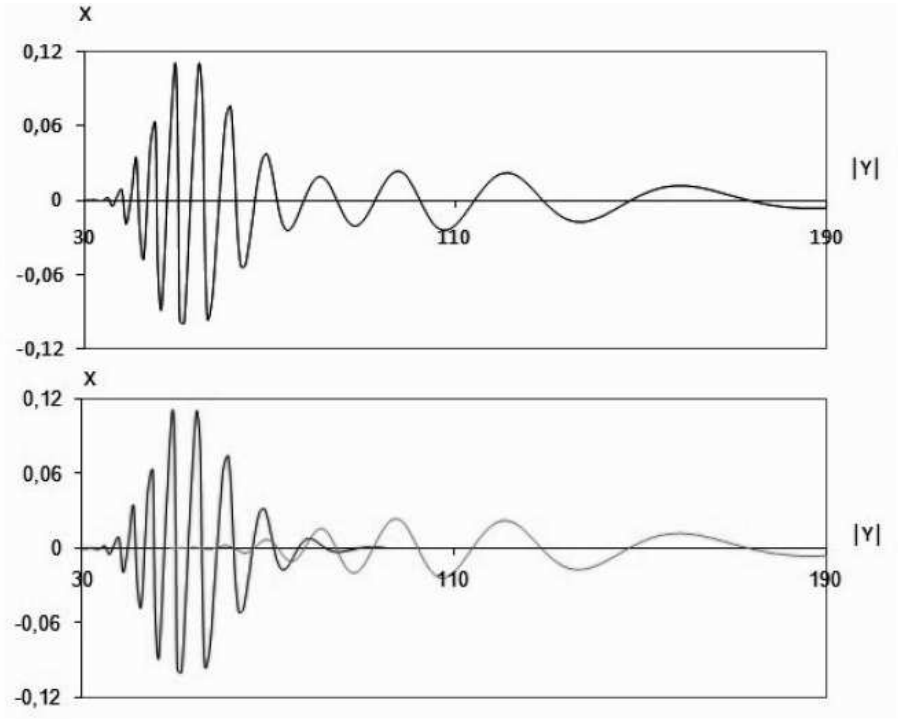

Figure 2: Instantaneous profiles of the waves (8.1) (upper panel), (8.2) (bottom panel, the curve on the left), and (8.3) (bottom panel, the curve on the right) at $\tau = 25$.

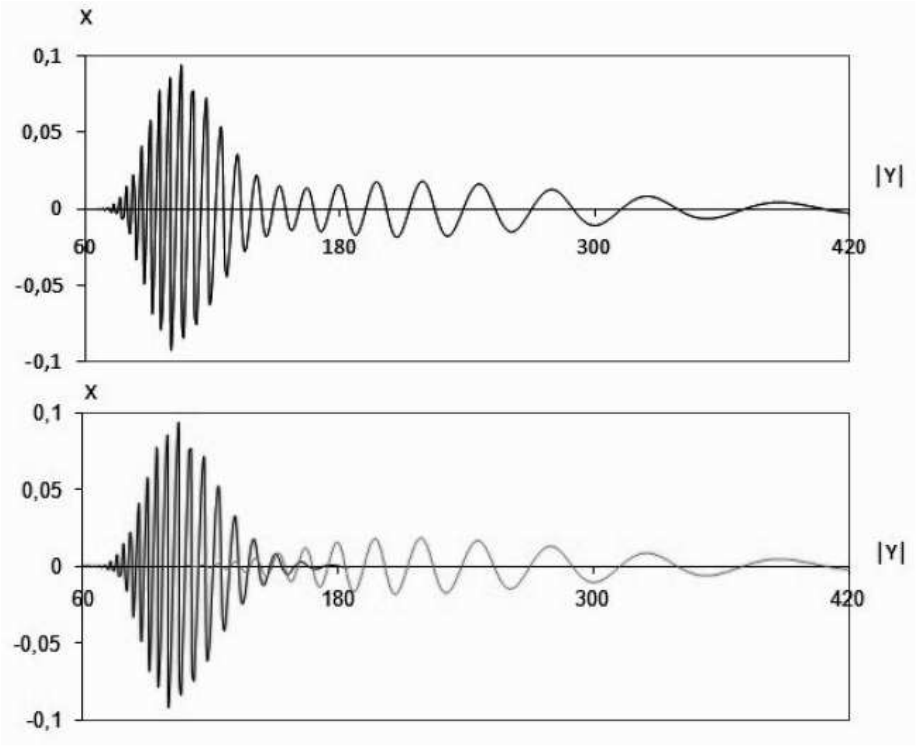

Figure 3: Same as Figure 2, but $\tau = 50$.

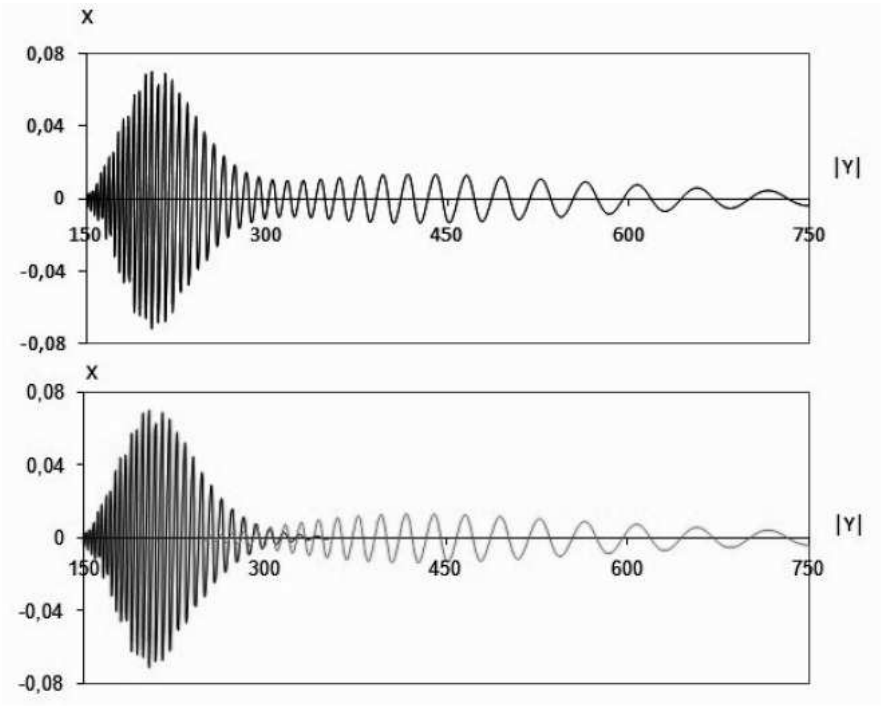

Figure 4: Same as Figure 2, but $\tau = 100$.

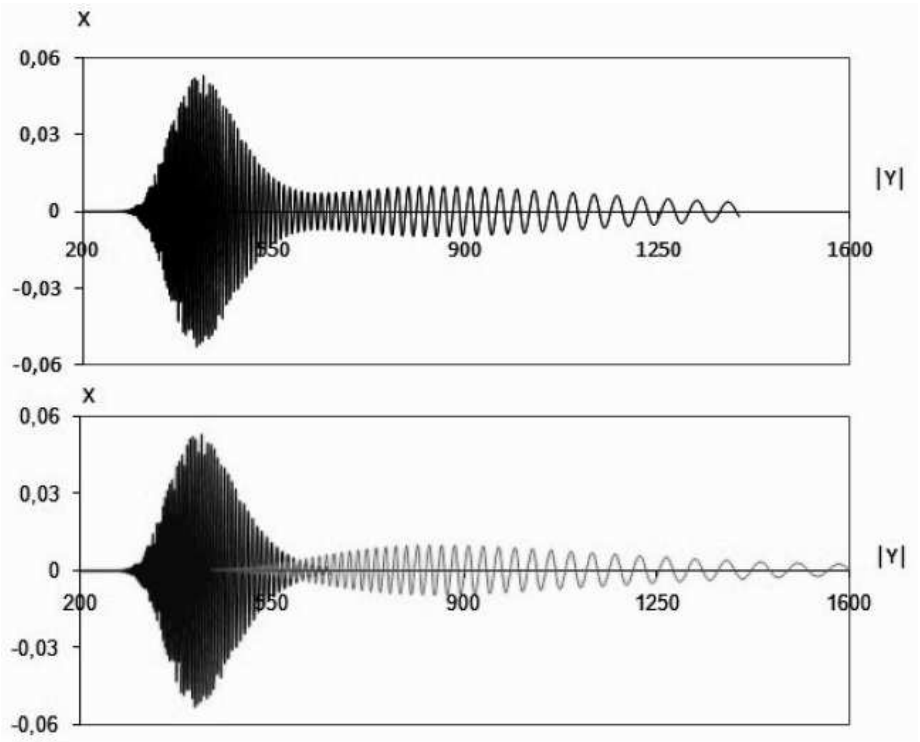

Figure 5: Same as Figure 2, but $\tau = 200$.

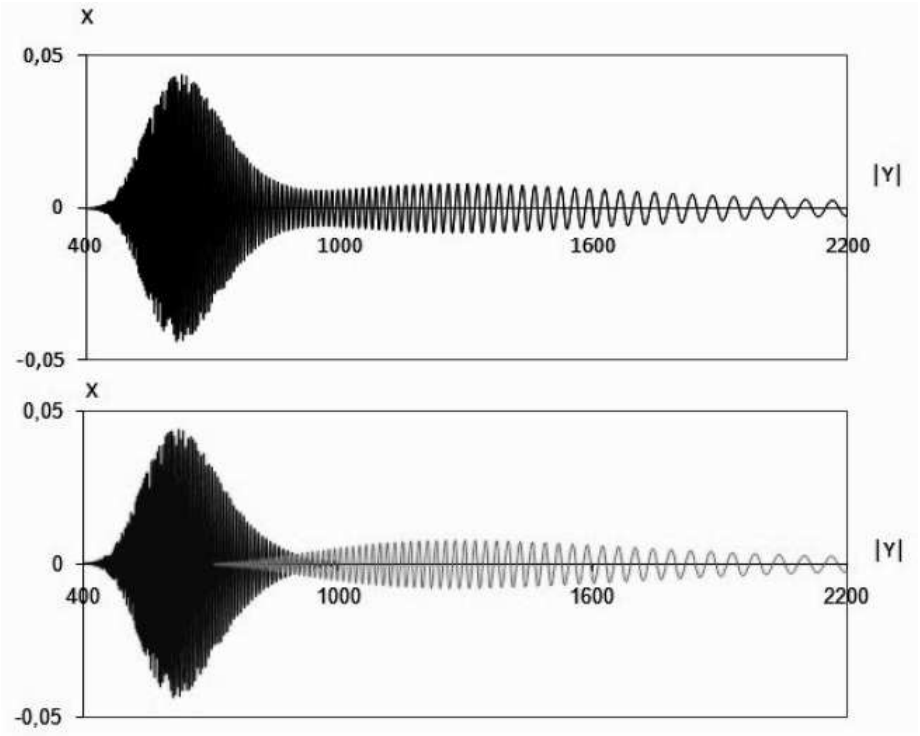

Figure 6: Same as Figure 2, but $\tau = 300$.

The figures show that the initial free surface displacement turns into two wave groups which run away from x-axis in opposite directions. From the figure we notice that with time the waves leave a region about the vertical plane $y = 0$. As there is no flow across the plane, the fluid motion would be unaffected if the plane was replaced by rigid barrier. From now on we will consider wave groups propagating in a fixed direction, say, along the semiaxis $y > 0$.

We note in passing that, in case of plane waves, the term 'wave group' means a system of waves in which the amplitude dies away on either side of the wave of maximum height; the term 'wave' means a wave-group's section which consists of one crest and the adjacent trough and is singled out by three successive zeros of the group; the level difference between a crest and the following or the preceding trough is referred to as the waveheight (or height of the wave); the term 'wave packet' means a wave group in which the amplitude dies away very quickly with distance from the wave of maximum height; figures 2 and 3 shows, that the waveheight of the wave of maximum height of the wave group (8.2) is about 0.21 at $\tau = 25$ and 0.18 at $\tau = 50$.

System of harmonic waves $x = \cos(ky - \omega t)$ on the free surface infinite in extent is not a wave group.

The wave group (8.1) is a nonlinear combination of wave packets (8.2) and (8.3). The figures show that the wave packets (8.2) and (8.3) propagate at different speeds: the horizontal distance between the crests of the waves of maximum height is approximately 70 at $\tau = 25$, 115 at $\tau = 50$, 260 at $\tau = 100$, 440 at $\tau = 200$, and 690 at $\tau = 300$.

The wave group (8.1) gradually disintegrates into its components (8.2) and (8.3), and each of the components doesn't affect the evolution of the another one.

The greater the number of a packet, the shorter the wavelength of the packet's carrier wave component and the slower the packet travels. The wavelength and velocity of simple harmonic waves on deep water are related in a similar way.

9. Infinitesimal linear wave packets: limit case of the nonlinear theory

Setting $y_1 = y/f$, substituting $y_1 f/(x - f)$ for $\tan\theta$ in $\hat{I}_{2m+1}$, letting $|f|$ tend to $+\infty$, we obtain the equations of the packet with number m as

$$x = W(y,t), \quad W = c \int_0^{+\infty} s^{2m+1} e^{-s^2/2} \cos(\frac{1}{2} s^2 y) \cos(ts)\, ds$$

where τ has been replaced by t and subscript 1 has been dropped.

Calculations show that the leading-order term $\Phi_0(x,y,t)$ for velocity potential and the function $W(y,t)$ satisfy equations

$$\frac{\partial W(y,t)}{\partial t} = \frac{\partial \Phi_0}{\partial n_-}, \qquad \frac{\partial \Phi_0}{\partial t_-} + W = 0 \tag{9.1}$$

where subscript "n" is used for the derivative in normal direction to the free surface $x = W(y,t)$, and equations (9.1) involve the partial derivatives at point x, y on the free surface; t is the non-dimensional time introduced in subsection 1.2.

By the way, note that at any value of f equation (3.3) may be rewritten as

$$\frac{\partial W}{\partial t} = \frac{\partial \Phi}{\partial n_-}$$

Equations (9.1) are the boundary conditions (ii) and (iii) named in the Introduction. If the conditions are moved from the free surface to the equilibrium plane $x = 0$, the normal derivative reads $\partial\Phi_0/\partial x|_{x=0}$.

We come to the following

Assertion 2:

As a limit case of the nonlinear theory, equations for infinitesimal deep water waves are obtained with boundary conditions on the evolving free surface, and the solution to the equations is found. If the boundary conditions are shifted from the evolving free surface to the equilibrium position of the surface, the equations reduce to equations of classical linear theory of infinitesimal waves.

10. Testing of the theory against experiments performed in a water tank

We use some results from wave pulse experiments presented by Feir [9] and Yuen & Lake [8] bearing in mind that the aim of Feir is to study the effects of finite amplitude of a wave group on the group shape and the frequency distribution over the group while the main purpose of the work by Yuen & Lake is to decide whether the predictions based on the Schrödinger equation correspond with experimental results.

The wave groups were generated in a tank equipped with a wavemaker. In [9] each wave pulse was recorded at one fixed point of the tank, while in [8] wave gauges located at the distances 5 ft, 10 ft, 15 ft, 20 ft, 25 ft, and 30 ft downstream of the wavemaker were used to record a wave group on the water surface so that the evolution of the wave group can be demonstrated.

The figure 7 is a reproduction of figure 1 shown in [8].

Evolution of three wave envelopes is shown in cases A, B and C corresponding to three initial profiles (given at $x = 0$) symmetric about their peaks: (A) envelope soliton, (B) a hyperbolic secant envelope, (C) a sine envelope of the same amplitude as in the case A; the amplitude scale of the hyperbolic secant envelope is reduced by a factor of 2.5 compared to the case A; in the three cases the carrier frequency of the wavemaker was 2 Hz; the experiments were performed in a water tank 3 feet deep. In figure 7 the wave envelopes propagate along the tank from the left to the right.

During the time interval of the observation, in case A, the shape of the envelope in the figure seems to be almost unchanged with time; in cases B and C, initial wave group gradually turns into a structure which consists of a

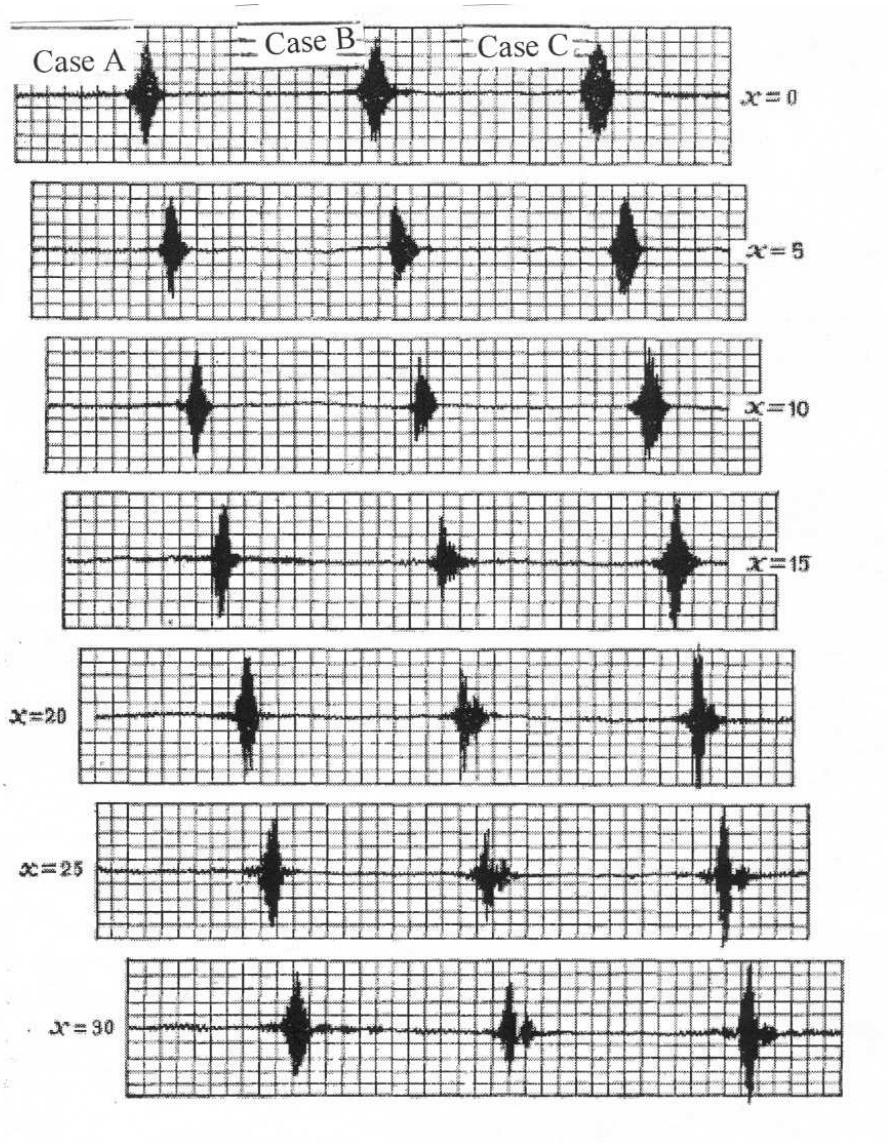

Figure 7: Evolution of three wave envelope pulses (reproduced from [8]).

relatively 'tall' wave packet following a 'low' one and long chains of waves of small amplitude in the front and in the rear of the system of packets. Formation of similar structures is shown in [8].

In [8] experimental measurements are not presented, actual dimensions of the envelopes as well as the ratio of vertical to horizontal scales and the individual wave profiles are not shown.

We can obtain an idea about the horizontal and vertical scales only for the initial envelope soliton (figure 7, case A, $x = 0$).

The shape of the envelope soliton is given by $x = a \operatorname{sech} u,\ u = \sqrt{2}k^2 a\, s$, $ka \approx 0.14$; $s = 0$ is the vertical axis of symmetry of the shape, a is the height of the envelope; maximum slope of the tangent to the envelope is reached at $u = 0.882$; coordinates of the point of tangency are $s = 32.14a,\ x = 0.7a$; at the level of the point, i.e., on the level of 0.7 of the envelop's height, the width of the envelope is nearly 64 times as great as the height.

But in figure 7, case A, at $x = 0$, the envelope's width on the level 0.7 of it's height is approximately of 0.2 of the height, so the ratio of the vertical scale to the horizontal scale is about 300.

Figure 8 shows the same profiles as the figures 2 - 6, but the horizontal scales are reduced significantly.

In figure 8, column A_1, the envelopes seem to be of the same height and the same width. The resemblance between columns B (figure 7) and B_1 (figure 8) is doubtless.

At $\tau = 25$ (figure 2, bottom panel, the curve on the left) the height of the packet (8.2) equals 0.1136, the packet's width at the level 0.7 of its height is equal to 6.6, 60 times as great as the height (as for envelope soliton with $ka = 0.144$). The length of the packet increases with time, while the height decreases (figures 2 - 6, bottom panels, the curves on the left; formation of a chain of waves of small amplitude in the front of the packet is demonstrated in the top panels).

In [9], a number of records of wave pulses are shown generated by a wavemaker oscillating at a carrier frequency of 2.5 Hz with amplitude varying slowly from zero to some maximum and back to zero; the range of the maximum amplitude of the wavemaker stroke was from 0.19 cm for the wave pulses of small amplitude to 1.5 cm for the pulses of large amplitude; in the records the range of maximum water surface displacement is from 1 mm to 10 mm. The maximum displacement of 6 mm at the distance of 8.53 m from the wavemaker is considered to be large (figure 2, p. 55.)

In [9], figure 1, p. 54, the record of a wave pulse was taken at the distance 8.53 m from the wavemaker. The upper part of the figure 1 shows the group of 25 individual waves which passes the gauge for 10 s. This means that the mean period of the waves is 0.4 s which equals to the wavemaker period. In the record, maximum water surface displacement is about 1 mm. Periods of the individual waves were measured and the results are shown in the lower part of the figure 1: in the figure, periods of 18 waves in the middle of the wave pulse are close to 0.4 s; periods of the waves at the ends of the pulse differ from the wavemaker period up to 20%.

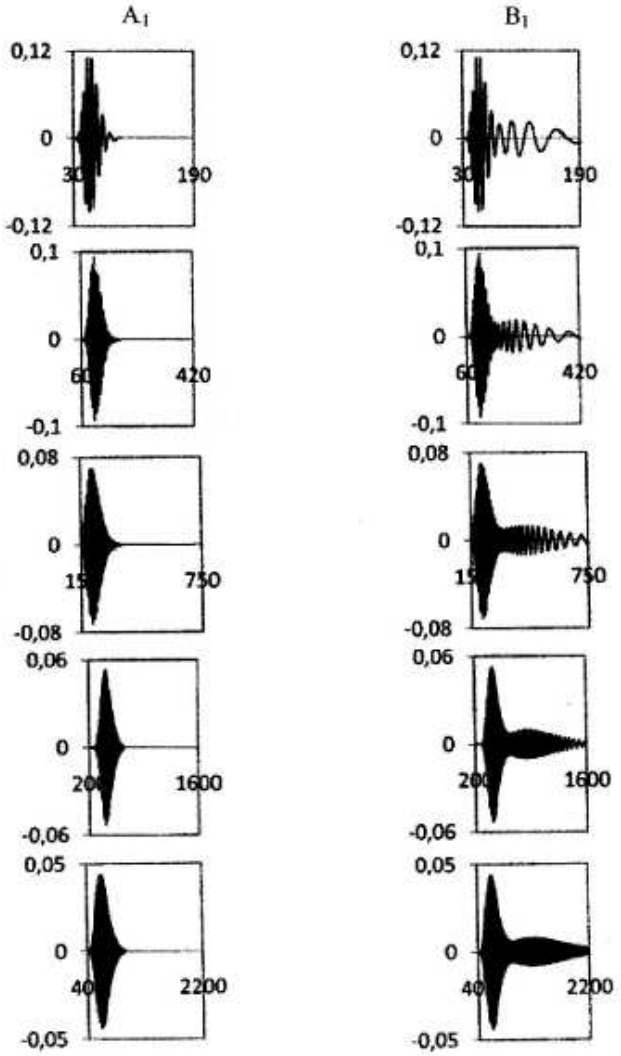

Figure 8: Same as figures 2 - 6 (top to bottom) at $\tau = 25,\ \tau = 50,\ \tau = 100,\ \tau = 200,\ \tau = 300$ respectively, but on reduced horizontal scale. Column A_1: profiles of packet (8.2), column B_1: profiles of packet (8.1).

Profile of packet (8.2) at $\tau = 100$ (figure 4, bottom panel, the curve on the left) is similar to the wave profile shown in [9], figure 1, p. 54: in figure 4, bottom panel, $160 < y < 300$, we can clearly see 25 individual waves.

The front of the wave of maximum height of packet (8.2) travels a distance of y_* from the origin $y = 0$ in a time t_*. Below for specific values of y_*, t_* and initial height of the packet, H_*, the following dimensional parameters of the packet are estimated:

L_* - the dimensional unit of length (see section 3);

$h_*(t_*)$ - the maximum height of the packet at the instant t_*;

V_* - the average speed of the packet during the travel time t_*;

v_* - the speed of the WMH at the instant t_*;

l_* - the length of WMH at the instant t_*;

l_{**} - the length of the packet at the instant t_*.

Algorithm for calculating values of the parameters may be summarized as follows:

Calculate the value of y_*/t_*^2 and then find the front of the wave of maximum height of packet (8.2) such that τ and $\tan\theta_f(\tau)$ satisfy equation (7.4); also find $\tan\theta_r(\tau)$, non-dimensional height $h(\tau)$ of the WMH, and $\tan\theta_f(\tau+\Delta\tau)$ at small $\Delta\tau$.

From equations $H_* = c\,L_*$ and $|f|L_*|\tan\theta_f(\tau)| = y_*$ find dimensional estimates for vertical L_* and horizontal $a = |f|L_*$ parameters of length (c is the non-dimensional height of the packet at $t = 0$). The height and the length of the WMH at the instant t_* are estimated as $h_*(t_*) = h(\tau)L_*$ and $l_* = a[|\tan\theta_f(\tau)| - |\tan\theta_r(\tau)|]$ respectively. The speeds are estimated by $V_* = y_*/t_*$, $v_* = \sqrt{0.5ag}\,[|\tan\theta_f(\tau+\Delta\tau)| - |\tan\theta_f\tau)|]/\Delta\tau$. Technique for estimating the length of the packet is shown below in example 1.

The estimates of packet parameters are independent of c (in (8.2) $c = 0.4$) and the estimate of a is independent of H_*. + In Feir [8] the lengths of the individual waves and the length of the wave pulse shown in figure 1 was not estimated, the travel time t_* from the wavemaker to the gauge and the maximum amplitude H_* of the pulse are not shown. It is reasonable to think that H_* is comparable with the maximum wavemaker stroke, and t_* is greater than 10 s, but not very.

Examples.

Example 1. At $y_* = 8.53$ m, $t_* = 27.4$ s, $H_* = 0.75$ cm, $g = 9,8$ m/s^2, $2y_*/(gt_*^2) = 0.0023$ and from equations (8.2) we obtain

$$\tau = 91, \quad \tan\theta_f(91) = 19.150, \quad \tan\theta_r(91) = 18.610, \quad \tan\theta_f(91.1) = 19.192$$

$$h(91) = 0.075, \quad L_* = 1.86 \text{ cm}, \quad a = |f|L_* = 0.445 \text{ m}$$

$$h_* = 1.4 \text{ mm}, \quad l_* = 0.24 \text{ m}, \quad V_* = 0.311 \text{ m/s}, \quad v_* = 0.620 \text{ m/s}$$

An estimate of instantaneous length of a wave packet based on a record of the packet depends on sensitivity of the wave amplitude gauge used for the record.

At the instant t_* the body of the packet is bounded by $y_{min} = |f|L_*\tan\theta_{min}$ and $y_{max} = |f|L_*\tan\theta_{max}$ where $\tan\theta_{min}$ and $\tan\theta_{max}$ are to be found from

equations (8.2) at obtained value of τ. The body of a packet includes waves with amplitudes greater than a preassigned level which depends on the gauge sensitivity.

Inequality $|x| > 0.01$ corresponds to waves with amplitude greater than 0.2 mm. At the instant t_* the waves are located in the interval $14.3\,a < y < 25.9\,a$ (at $\tau = 91$ $\tan\theta_{min} = 14.3$, $\tan\theta_{max} = 25.9$). The length of the interval is estimated as $l_{**} = (25.9 - 14.3) \cdot 0.45$ m $= 5.2$ m.

In the interval $15\,a < y < 25\,a$ the inequality $|x| > 0.02$ holds. At the instant t_* the length of the interval is estimated as $l_{**} = 10 \cdot a = 4.5$ m.

At the instant t_* in the interval $15.5\,a < y < 22.3\,a$ inequality $|x| > 0.03$ is satisfied, so amplitudes of the waves in the interval are greater than 0.6 mm. The length of the interval is estimated as $l_{**} = 6.8 \cdot a = 3.0$ m.

Depending on the preassigned amplitude level, one of the three values may be taken as the estimate of the packet length at the instant t_*.

The above estimates of the average speed of the packet and speed of the wave of maximum height equal to estimates of group and phase velocities respectively based on linear theory for waves of infinitesimal amplitude: at phase velocity of 0.62 m/s of sinusoidal carrier wave of a packet the carrier frequency is $\omega = 15.8\ \mathrm{s}^{-1}$, the wavenumber is $k = \omega^2/g = 25.47\,\mathrm{m}^{-1}$, the group velocity is $v = 0.5\omega/k = 0.31$ m/s.

Example 2. At $y_* = 8.53$ m, $t_* = 24$ s, $H_* = 0.5\,$cm, $g = 9.8\ \mathrm{m/s}^2$, $2y_*/(gt_*^2) = 0.0030$ we obtain

$$\tau = 70,\quad \tan\theta_f(70) = 14.765,\quad \tan\theta_r(70) = 14.227,\quad \tan\theta_f(70.1) = 14.807$$

$$h(70) = 0.084,\quad L_* = 1.25\text{ cm},\quad a = |f|L_* = 0.578\text{ m}$$

$$h_* = 1.05\text{ mm},\quad l_* = 0.31\text{ m},\quad V_* = 0.355\text{ m/s},\quad v_* = 0.707\text{ m/s}$$

Example 3. At $y_* = 8.53$ m, $t_* = 28.8$ s, $H_* = 0.7\,$cm, $g = 9.8\ \mathrm{m/s}^2$, $2y_*/(gt_*^2) = 0.0021$ we obtain

$$\tau = 100,\quad \tan\theta_f(100) = 20.990,\quad \tan\theta_r(100) = 20.450,\quad \tan\theta_f(100.1) = 21.032$$

$$h(100) = 0.072,\quad L_* = 1.75\text{ cm},\quad a = |f|L_* = 0.406\text{ m}$$

$$h_* = 1.3\text{ mm},\quad l_* = 0.22\text{ m},\quad V_* = 0.296\text{ m/s},\quad v_* = 0.592\text{ m/s}$$

The section $170 < y < 250$ in figure 4 (bottom panel, the curve on the left) of the packet includes only waves with amplitudes greater than 0.2 mm. The length of the packet is estimated as $(25 - 17) \cdot a = 3.2$ m.

The examples show that the average speed of the packet of finite amplitude during the travel time t_* is a half of the speed of the WMH at the instant t_*; exactly the same relationship exists between group and phase velocities in linear theory of deep water waves of infinitesimal amplitude; the average speed of the packet (8.2) and the speed of the WMH are equal, respectively, to the group and phase velocities of a linear wave packet provided that sinusoidal carrier wave of the linear packet and the wave of maximum height of nonlinear packet (8.2) have the same wavelength.

The reason for the relationship between the four speeds is that (by their definitions) the speeds are independent of the amplitude of packet (8.2).

The assertion 2 and the examples lead to

Assertion 3:

The average speed of a nonlinear wave packet of finite amplitude during a travel time t_* is a half of the speed of the packet's wave of maximum height at the instant t_*; the average speed of the nonlinear packet and the speed of the wave of maximum height are equal, respectively, to the group and phase velocities of a linear wave packet provided that sinusoidal carrier wave of the linear packet and the wave of maximum height of the nonlinear packet have the same wavelength.

Now we return to the pulse experiment by Feir. In [9], the length of the wave pulse shown in figure 1, the travel time t_* from the wavemaker to the gauge and the maximum amplitude H_* of the pulse are not shown. Nevertheless, the first two quantities can be estimated as follows: by the linear theory, a wave packet with carrier frequency of 2.5 Hz travels at the group velocity of 0.31 m/s. This suggests that the length of the wave pulse is $0.31\ \text{m/s} \cdot 10\ \text{s} = 3.1$ m, and the travel time from the wavemaker to the gauge is about 27.5 s.

These values of the travel time and length of the experimental wave pulse are in good agreement with the estimates obtained in the three examples above.

11. About higher-order approximations to the full nonlinear problem.

Under what conditions the solution of the leading-order equations gives a reasonable approximation of solution for full nonlinear problem?

The usual technical work with expansions leads to a sequence of systems of linear nonhomogeneous equations. Every nonhomogeneous system of the sequence involves terms corresponding to applied "forces" or "sources". The corresponding homogeneous equations are identical. It is impossible to answer the question unless the exact solution of the leading-order equations is studied for arbitrary initial conditions and arbitrary "force" -terms.

It can be shown that under boundary conditions (3.5) the "force" -terms have the form $\cos^2\theta \cdot F(\theta, t)$.

Having expanded the function $F(\theta, t)$ in a trigonometric series of the form

$$F(\theta,t) = \sum_{k=1}^{+\infty} \alpha_k(t)\cos(2k\theta) + \beta_k(t)\sin(2k\theta)$$

$$\sum_{k=1}^{+\infty} \sqrt{{\alpha_k}^2 + {\beta_k}^2} < +\infty.$$

we can obtain nonhomogeneous linear integrodifferential equations just of the type considered in [5] where the exact solution to the nonhomogeneous equations were obtained.

The solution shows that the "input" and the "output" of the nonhomogeneous linear equations (i.e., the applied "forces" and the solution) are related by a bounded operator.

This means that the exact solution of the leading-order equations give a reasonable approximation to the solution of the full nonlinear problem for small values of the parameter ε.

We are able to construct higher-order approximaations to the solution of the full nonlinear problem, provided the "force" -terms are actually expanded in the trigonometric series similar to that shown above.

Appendix A

Solution to the leading-order equations (4.1), (4.2) is sought by expanding unknown functions in trigonometric series:

$$W_0(\theta,t) = \cos^2\theta \sum_{k=1}^{+\infty} [\hat{a}_k(t)\cos(2k\theta) + \hat{b}_k(t)\sin(2k\theta)]$$

$$\nu_0(\theta,t) = \sum_{k=0}^{+\infty} [\hat{\rho}_k(t)\cos(2k\theta) + \hat{e}_k(t)\sin(2k\theta)] \qquad (A1)$$

In order to simplify matters, initial values of the coefficients are assigned as

$$\hat{a}_n(0) = a_n, \quad \hat{a}_k(0) = 0 \ \text{ for } \ k \neq n \quad \hat{b}_k(0) = \hat{\rho}_k(0) = \hat{e}_k(0) = 0 \qquad (A2)$$

Inserting (A.1) in the equations (4.1), (4.2), making use of the expressions (4.3) for operator $H(F)$, and equating coefficients of $\cos(2k\theta)$, we obtain the following differential equations for coefficients of the series (A.1):

$$\frac{d\hat{a}_k}{dt} = -\frac{k}{|f|}\hat{\rho}_k, \quad \frac{d\hat{\rho}_k}{dt} = \frac{1}{2}\hat{a}_{k-1} + \hat{a}_k + \frac{1}{2}\hat{a}_{k+1}, \quad k = 0,\, 1,\, 2,\, \ldots \qquad (A3)$$

Equations (A.3) are derived using formulas (4.3) at small values of $|\sigma|$. Letting σ tend to 0, we find one-sided limits shown in (4.1) and (4.2).

Exact solution to the initial value problem (A.3), (A.2) is given by

$$n\hat{a}_k(t) = (-1)^k(-1)^n 2a_n \int_0^{+\infty} x^3 e^{-x^2} L_{k-1}^{(1)}(x^2) L_{n-1}^{(1)}(x^2)\cos(\tau x)\,dx$$

$$\frac{k}{|f|}\hat{\rho}_k = (-1)^k(-1)^n 2a_n \int_0^{+\infty} x^4 e^{-x^2} L_{k-1}^{(1)}(x^2) L_{n-1}^{(1)}(x^2)\sin(\tau x)\,dx \qquad (A.4)$$

This can be verified by substituting (A.4) into equations (A.3) (formula (5.8) and the orthogonality integral for Laguerre polynomials should be taken into account).

Equations (A.1), (A.4) lead to expressions (5.3), (5.5) for $C_n(\tau,\theta)$ and $H_n(\tau,\theta)$. Expressions (5.4) and (5.6) for $S_n(\tau,\theta)$ and $G_n(\tau,\theta)$ can be obtained in the similar way.

REFERENCES

1. Zakharov, V.E.: Stability of periodic waves of finite amplitude on the surface of a deep fluid, J. App. Mech. Tech. Phys. 9, 190-194 (1968). (Translated from Russian)

2. Hasimoto, H., Ono, H.: Nonlinear modulation of gravity waves, J. Phys. Soc. Jap. 33, 805-811 (1972).

3. Davey, A.: The propagation of a weak nonlinear wave, J. Fluid Mech. 53, 769-781 (1972).

4. Yuen, H.C., Lake, B.M.: Nonlinear Deep Water Waves: Theory and Experiment, Phys. Fluids. 18, 956-960 (1975).

5. Zakharov, V.E., Shabat, A.B.: Exact theory of two-dimensional self-focusing and one-dimensional self-modulating waves in nonlinear media, Soviet Phys. JETF. 65, 997-1011 (1972). (Translated from Russian)

6. Mindlin, I.M.: Nonlinear waves in two-dimensions generated by variable pressure acting on the free surface of a heavy liquid, J. Appl. Math. Phys. (ZAMP) 55, 781-799 (2004).

7. Mindlin, I.M.: Integrodifferential Equations in Dynamics of Heavy Layered Liquid, Nauka∗Fizmatlit, Moscow,(1996) (Russian).

8. Yuen, H.C., Lake, B.M.: Nonlinear dynamics of deep-water gravity waves. In: Chia-Shun Yih (Ed.), Advances in applied mechanics, 22, Academic press, New York ∗ London, 67-229 (1982).

9. Feir, J.E.: Discussion: Some results from wave pulse experiments, In: A discussion on nonlinear theory of wave propagation in dispersive systems, Proc. R. Soc. 299 London, 54-58 (1967).

10. Show, R.P.: Boundary integral equation methods applied to water waves. In: T.A.Cruze, F.J. Rizzo (Ed.), Boundary-integral equation method: computational applications in applied mechanics, ASME, Rensselaer Polytechnic Institute, June 23-25,. AMD-vol. 11 (1975)

11. Suetin, P.K. Classical Orthogonal Polynomials, Nauka, Moscow, (1964) (Russian).